Available online at www.sciencedirect.com
SCIENCE DIRECT®
Bioelectrochemistry 59 (2003) 65–72
Bioelectrochemistry
www.elsevier.com/locate/bioelechem

Nanostructured platinum-lipid bilayer composite as biosensor

Jian-Shan Ye[a], Angelica Ottova[b], H. Ti Tien[b], Fwu-Shan Sheu[a,c,*]

[a] Department of Biological Sciences, National University of Singapore, 14 Science Drive 4, Singapore 117543, Singapore
[b] Department of Physiology, Membrane Biophysics Laboratory, Michigan State University, 2201 Biomedical and Physical Sciences Building, East Lansing, MI 48824, USA
[c] The University Scholars Programme, National University of Singapore, 10 Kent Ridge Crescent, Singapore 119260, Singapore

Received 12 August 2002; received in revised form 12 December 2002; accepted 8 January 2003

Abstract

The present work describes the preparation of supported bilayer lipid membrane (s-BLM) doped with metal nanoparticles for the design of biosensors. Platinum (Pt) nanoparticles were deposited through s-BLM to build a hybrid device of nanoscale electrode array by potential cycling in 1 mM K_2PtCl_6 solution containing 0.1 M KCl. The properties of Pt nanoparticle-doped s-BLM composite were then characterized by cyclic voltammetry, electrochemical impedance spectroscopy (EIS) and atomic force microscopy (AFM). Our results showed that Pt nanoparticles grew in voids of the s-BLMs, through which the underlying glassy carbon (GC) electrode was connected, with maximum length extended out of the lipid membrane around 40 nm. Doping of Pt nanoparticles through s-BLM increased the membrane capacitance and decreased the membrane resistance of s-BLM. Pt nanoparticles array in s-BLM electrocatalyzed the reduction of oxygen (O_2) in phosphate buffer solution (PBS). Practical application of Pt nanoparticle-doped s-BLM for the construction of glucose biosensor was also demonstrated in terms of its dose–response curve, stability and reproducibility. Thus, lipid membrane doped with Pt nanoparticles is a novel electrode system at nanoscale that can penetrate through the insulating membrane to probe molecular recognition and catalytic events at the lipid membrane–solution interface.

Keywords: Nanoparticles; Supported bilayer lipid membrane (s-BLM); Cyclic voltammetry; Electrochemical impedance spectroscopy; Biosensor

1. Introduction

The supported bilayer lipid membrane (s-BLM) has attracted considerable interests in recent years due to its many potential applications as an electrochemical biosensor and in molecular devices [1–3]. Bilayer lipid membranes (BLMs) have been used in various experimental paradigms as models of actual living cell membranes [4–6]. BLMs provide a natural environment for embedding a host of compounds such as proteins, receptor, membrane/tissue fragments, and even whole cells under nondenaturing conditions and in a well-defined orientation. The lipid bilayer acts as a very thin electric insulator, as a framework for antigen–antibody binding, as a bipolar electrode for redox reactions and as a reactor for energy conversion.

To study the photoelectrical and electrochemical properties as well as for practical applications, a BLM containing semiconductor polycrystallites (semiconductor nanoparticles) has been successfully prepared [1,7]. For example, CdS crystallites can be formed in situ in the pores of a polycarbonate membrane separating two aqueous solutions. When the CdS-membrane was irradiated, open-circuit photopotentials up to 500 mV were obtained. A number of substances, such as Cu, CuS, CdS, FeS and AgBr having typical metallic or semiconducting features, have been deposited onto the surface of BLMs [1,7,8]. Nanoparticle-coated BLMs show very good stability in comparison with unmodified BLMs, which usually lacked satisfactory durability. Metallic or semiconducting layers deposited onto the BLM surface can serve as electrodes directly contacting the membrane which eliminate electrolytic contact with the lipid bilayers and may be useful in the development of biomolecular electronic devices [1,7].

Similar studies in semiconductor containing BLMs have been reported [8]. To prepare semiconductor containing BLMs, H_2S and appropriate metal ion precursors were added

* Corresponding author. Department of Biological Sciences, National University of Singapore, 14 Science Drive 4, Singapore 117543, Singapore. Tel.: +65-68742857; fax: +65-67792486.
E-mail address: dbssfs@nus.edu.sg (F.-S. Sheu).

1567-5394/03/$ - see front matter © 2003 Elsevier Science B.V. All rights reserved.
doi:10.1016/S1567-5394(03)00003-3

onto bathing solutions on opposite sides of the BLM. Subsequent to the injection of H_2S, the first observable change was the appearance of fairly uniform white dots on the blank film. These dots rapidly moved around and grew in size, forming islands that then merged with each other and with a second generation of dots, which ultimately led to continuous film that continued to grow in thickness. The semiconductor penetration depth onto the BLM can be assessed by an equivalent RC circuit. Metallic or semiconducting layers formed onto the BLMs may have potential utilization in membrane mimetic chemistry [1–6]. The deposition of nanoparticles onto the surface of BLMs or inside the BLMs can drastically alter the mechanical, electrical and optical properties of the BLM. Nanoparticles doped through the s-BLMs may perform as an array of nanoelectrodes, while s-BLMs retain biocompatible microenvironment. However, the direct deposition of nanoparticles through s-BLMs has not been reported. Thus, in order to investigate the properties of nanoparticle-doped BLMs, we deposited Pt nanoparticles through the s-BLM by electrochemical method. Details of the preparation, characterization and possible application of this nanostructured Pt-lipid bilayer composite are described in the experimental section below.

2. Materials and methods

2.1. Reagents

L-α-phosphatidylcholine, dimyristoyl (DMPC) (≥99%, TLC), glucose oxidase (GOx) (EC 1.1.3.4, 40,300 units/g solid, Type II-S from *Aspergillus niger*), D-(+)-glucose (≥99.5%, HPLC), $K_3[Fe(CN)_6]$, $K_4[Fe(CN)_6]$ and K_2PtCl_6 were purchased from Sigma. Chloroform (analytical grade) was from J.T. Baker. Purified oxygen (≥99.8%) was from Soxal (Singapore). Phosphate buffer solution (PBS) contains: 8 g/l NaCl, 0.2 g/l KCl, 1.44 g/l Na_2HPO_4, 0.24 g/l KH_2PO_4 with pH 7.4. Deionized water was used throughout.

2.2. Electrochemical system and instrumentation

All electrochemical measurements and impedance spectroscopy were performed on an electrochemical workstation (CHI 660A, CH Instruments, USA). The three-electrode system consisted of the modified electrode as the working electrode, a KCl-saturated Ag/AgCl reference electrode and a platinum (Pt) wire auxiliary electrode. For the investigation of the structure of s-BLM with and without Pt nanoparticles, electrochemical impedance spectroscopy (EIS) was applied to measure the basic electrical properties such as membrane resistance and membrane capacitance. Impedance measurements were taken in the frequency range of 0.1 Hz to 100 KHz. A 5-mV amplitude sine with DC potential 0 V (with respect to the open-circuit potential wave) was applied between the working and reference electrode.

Amperometric experiments were performed at +0.40 V with PBS as supporting electrolyte. During the amperometric experiment, the solution was kept stirred at 300 rpm by a magnetic stirring bar.

2.3. Electrode preparations

DMPC was dissolved in chloroform to give a final concentration of 2 mg/ml. Prior to s-BLM formation, a glassy carbon (GC, 3-mm diameter from CH Instruments) was polished repeatedly with 1.0, 0.3, and 0.05 μm alumina slurry, followed by successive sonication in deionized water and acetone for 5 min. The electrode was dried in air. Then an 8-μl aliquot of the lipid solution was dropped onto the surface of the electrode by a microsyringe. Chloroform was evaporated gradually in air. The lipid-coated electrode was transferred into PBS, in which s-BLM was formed spontaneously (DMPC-modified electrode was described as DMPC/GC).

To electrochemically deposit Pt particles though s-BLM, DMPC/GC electrode was immersed in 1 mM K_2PtCl_6 solution containing 0.1 M KCl, and the potential cycle was between +0.30 and −0.70 V at a scan rate of 50 mV/s (Pt particle-modified DMPC/GC electrode was described as Pt@DMPC/GC). For comparison without the s-BLM formation, GC electrode was immersed in 1 mM K_2PtCl_6 solution containing 0.1 M KCl, and the potential cycle was between +0.30 and −0.70 V at a scan rate of 50 mV/s. (Pt particle-modified GC electrode was described as Pt/GC).

For the preparation of enzyme electrode, Pt/GC, DMPC/GC or Pt@DMPC/GC was soaked in PBS containing 2 mg/ml GOx for 12 h at 4 °C and was then gently washed with PBS. (The enzyme electrode was described as GOx/Pt/GC, GOx/DMPC/GC or GOx/Pt@DMPC/GC, respectively).

2.4. Atomic force microscopy (AFM) and scanning electron microscopy (SEM) imaging

AFM analysis of Pt nanoparticles deposited through s-BLM was carried out using nanoSurf easyScan™ AFM (Nanosurf, Switzerland). AFM images were taken in air in the noncontact mode and were examined at least in three different sites in given samples. SEM of Pt particles deposited at bare GC electrode was taken at FEG SEM (XL 30, Philips) operating at 5 KV.

3. Results

3.1. Formation and characterization of s-BLM and Pt hybrid s-BLM on GC electrode by cyclic voltammetry

Fig. 1(a) shows the cyclic voltammogram (CV) of bare GC electrode in 5 mM $K_3[Fe(CN)_6]$ solution containing 1 M KCl. After immersing DMPC lipid-coated GC electrode in

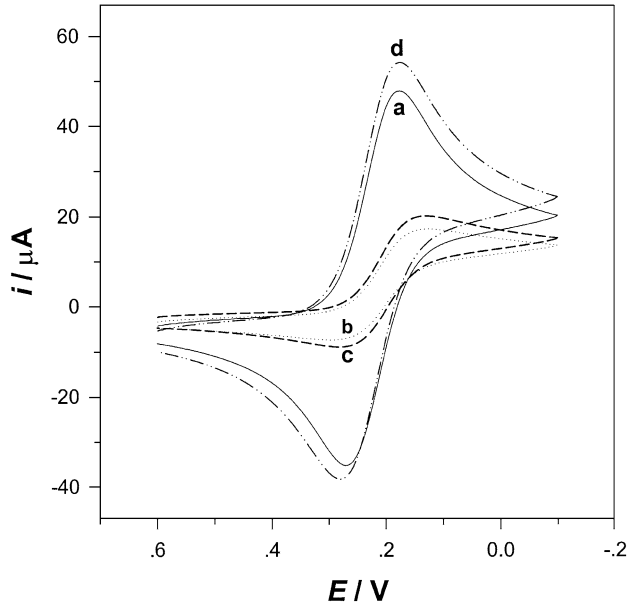

Fig. 1. Cyclic voltammograms of electrodes in 5 mM $K_3[Fe(CN)_6]$ solution containing 1 M KCl. (a) Bare GC electrode (solid line), (b) DMPC/GC electrode (dotted line), (c) Pt@DMPC/GC electrode (dash line), or (d) Pt/GC electrode (dash–dotted line). Scan rate: 50 mV s^{-1}.

PBS for 10 min, the electrode was put in 5 mM $K_3[Fe(CN)_6]$ solution containing 1 M KCl to obtain its CV as shown in Fig. 1(b). Compared to the CV of GC electrode, which has a large redox current for cathodic and anodic waves of $K_3[Fe(CN)_6]$, the CV of DMPC/GC shows a decrease in the current response, demonstrating that s-BLM has been formed on the surface of GC to insulate the electrode. Such insulation reduces redox reaction of $K_3[Fe(CN)_6]$ that occurs on the surface of the s-BLM-coated GC electrode [9,10]. In comparison, after Pt has been successfully deposited through s-BLM [Fig. 1(c)] or directly deposited onto the GC electrode [Fig. 1(d)], the current response of respective CV could be increased, indicating the enhancing effect of the Pt nanoparticles on the electron transfer to the electrodes. In the presence of BLM on the surface of GC electrode, the BLM blocked the access of $Fe(CN)_6^{3-}$ to the electrode surface. On the other hand, when the Pt particles were deposited through the bilayer membrane, the current response of $K_3[Fe(CN)_6]$ was increased to 21.2 μA. Thus, the current response was enhanced by Pt particles deposited through the s-BLM.

Because a perfect formation of the s-BLM is ion-impermeable [9], the redox ions cannot therefore diffuse through the lipid layer. As a result, the s-BLM-modified electrode is inert to most electroactive species in the bathing solution [9,11]. Nonetheless, at the DMPC/GC electrode, the inhibition of the current response of ferricyanide by the DMPC film at GC electrode is not particularly strong, compared to the s-BLM film on stainless steel electrode [9] and silver electrode [11]. Moreover, the peak-to-peak potential difference is practically equal to that on the bare GC electrode. This indicates that (1) the DMPC film is loosely packed on the surface of the GC electrode and (2) the electron transfer proceeds through the pinholes in the lipid film [12,13]. According to the model proposed by Amatore et al. [12], the pinholes in the lipid film can be regarded as a microarray electrode and the cyclic voltammograms characterized by mass transfer should be observed in the ferricyanide solution. s-BLMs at the surface of GC electrode as in this case and in another report [10] are consistent with Amatore's model. We attribute the reason of the existence of pinholes in the DMPC film at the GC electrode as follows. A self-assembled lipid bilayer, if formed on freshly cut metallic substrate in aqueous media, is devoid of pinholes owing to its liquid crystalline state; it routinely raises the resistance of the metal by several orders of magnitude [1]. On the other hand, the GC is a disordering material with some inherent pits, presumably from gas bubbles remaining in the bulk material during the fabrication of GC as indicated by Raman spectroscopy [14]. Furthermore, polishing during the preparation leads to an increase of disordered ratio due to mechanical disordering of the GC structure [15]; the polished GC surface exhibits a shoulder in the region of 286.5–288 eV in X-ray photoelectron spectroscopy [14], which is commonly attributed to carbon atoms associated with surface oxides. As a result, the pinholes exist in s-BLMs at the surface of GC due to the disordering structure and the surface oxides. Given the fact of the pinholes existence in the DMPC/GC electrode, these pinholes may provide a unique advantage that is suitable for the nanoscale sites for electrochemical deposition of electrocatalytic nanoparticles in the present study.

3.2. Electrochemical deposition of Pt nanoparticles through GC-supported lipid membranes

The electrochemical deposition of Pt nanoparticles through s-BLM was achieved by applying potential cycling onto the DMPC/GC electrode in 1 mM K_2PtCl_6 solution containing 0.1 M KCl as shown in Fig. 2A(a). When the potential scanning was applied from +0.30 to −0.70 V, there was evidently an increase in current starting from −0.1 V, showing that Pt particles can be deposited starting from the first scanning. The arrows in Fig. 2A(a) indicate the trends of the currents during the CVs, which demonstrate that Pt particles have been continuously deposited through the lipid membrane. For comparison, the deposition of Pt particles at the surface of the bare GC electrode was studied as shown in Fig. 2A(b). At the bare GC electrode, the current increased from +0.10 V. These results showed that Pt was more easily deposited onto the bare GC than through the lipid bilayers. Furthermore, the current response in the first scan at the bare GC is 2.5 times bigger than that of the DMPC/GC. This indicated that s-BLM mostly blocked the access of $PtCl_6^{2-}$ to the surface of GC. As a result, less Pt was deposited at DMPC/GC. The current response decreased during the consecutive cycles,

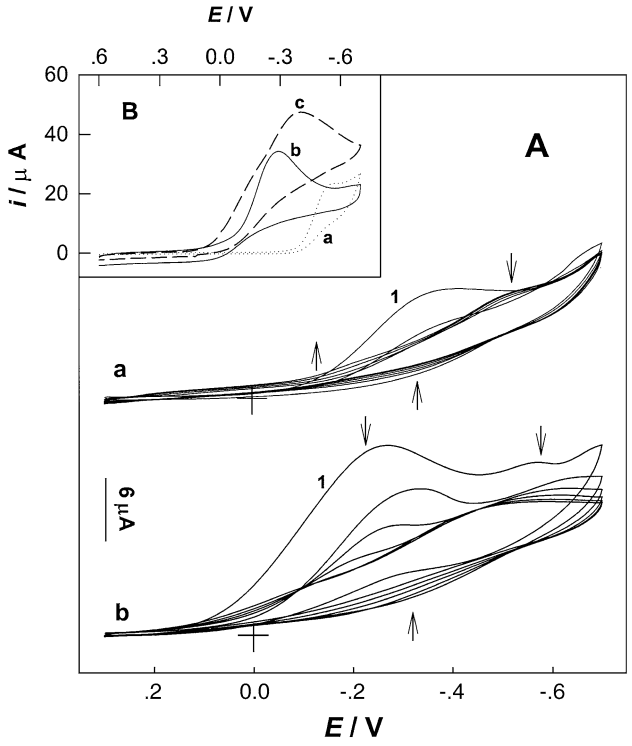

Fig. 2. (A) Electrochemical deposition of (a) Pt nanoparticles through lipid bilayers or (b) Pt particles at bare GC. Cyclic voltammograms of (a) DMPC/GC electrode or (b) bare GC electrode in 1 mM K_2PtCl_6 solution containing 0.1 M KCl. Arrows indicate the trend of currents during the potential cycling. 1 marks the first scan. (B) Cyclic voltammograms of (a) DMPC/GC electrode (dotted line), (b) Pt@DMPC/GC electrode (solid line), or (c) Pt/GC electrode (dashed line) in O_2-saturated PBS, respectively. Scan rate: 50 mV s^{-1}.

suggesting that less Pt was deposited in the subsequent cycles.

To make use of the Pt particles deposited through the s-BLM as a biosensor, we examined the electrocatalytic activity of Pt@DMPC/GC towards the reduction of O_2. In O_2-saturated PBS, the reductive current of O_2 was observed when the potential was more negative than -0.40 V on a DMPC/GC electrode as shown in Fig. 2B(a) (dotted line). On Pt@DMPC/GC electrode, the current response for O_2 reduction increases dramatically and the peak potential shifts positively to -0.291 V [Fig. 2B(b), solid line]. The increase of peak current and the positively shifted potential showed that Pt nanoparticles deposited through s-BLM made it easier to electrocatalyze the reduction of O_2. The result also indicated that Pt nanoparticles might penetrate through the bilayer lipid membrane and serve as nanoelectrodes that were electrically connected to the underlying GC substrate electrode. The peak currents on Pt@DMPC/GC electrode depended linearly on the square root of the scan rate over the range of 0.01 to 0.5 V/s, which suggested that O_2 was undergoing a diffusion-controlled process at Pt@DMPC/GC electrode. The peak current could be eliminated when the PBS was bubbled with N_2 gas (data not shown), confirming that the current response in Fig. 2B was due to the electrocatalytic reduction of O_2. An increase of current response for O_2 reduction at Pt/GC [49.6 μA, Fig. 2B(c)] was observed as compared to that of at Pt@DMPC/GC [38.2 μA, Fig. 2B(b)]. In 5 mM $K_3[Fe(CN)_6]$ solution containing 1 M KCl, the current response at Pt/GC was 55.2 μA [Fig. 1(d)], while it was 19.5 μA at Pt@DMPC/GC [Fig. 1(c)]. This further indicated that (a) $K_3[Fe(CN)_6]$ could not penetrate through s-BLM and only responded to Pt nanoparticles outside s-BLM, whereas (b) O_2 could penetrate through s-BLM and responded at Pt nanoparticles both outside and inside s-BLM to give rise to bigger redox currents.

3.3. The impedance measurements of GC-supported lipid membranes with and without Pt nanoparticles

EIS is an effective method for probing the feature of surface-modified electrode [2,3,10,11,16,17]. For example, Wiegand et al. [3] characterized the electrical properties of s-BLMs on semiconductor and gold surfaces in details. They introduced a novel equivalent circuit model for data evaluation, which accounted the deviation of the impedance response of s-BLMs from that of an ideal RC element. In the present study, AC impedance of DMPC/GC and Pt@DMPC/GC were investigated at AC frequency from 0.1 Hz to 100 KHz to get more information of the properties of s-BLM when doping with metal nanoparticles. For the sake of giving more detailed information about the impedance properties of the membranes, a modified Randles equivalent circuit [10] (inset of Fig. 3B) was chosen to fit the measured results. The total impedance was determined by several parameters: (1) electrolyte resistance, R_s; (2) the lipid bilayer capacitance, C_{dl}, which consisted of the unmodified GC electrode (C_{GC}) and a capacitance originated from the DMPC membrane (C_m) on the surface of the electrode [10]; (3) charge transfer resistance, R_{ct}; and (4) Warburg element, Z_w. The complex impedance can be presented as the sum of the real, Z_{re}, and imaginary, Z_{im} components that originate mainly from the resistance and capacitance of the cell.

Fig. 3 illustrates the results of impedance spectroscopy on (A) a bare GC electrode and (B) a modified electrode with and without Pt nanoparticles in the presence of equimolar 10 mM $[Fe(CN)_6]^{3-/4-}$ containing 0.1 M KCl. It can be seen from Fig. 3A that the bare GC electrode exhibited an almost straight line that was characteristic of a diffusional limiting step of the electrochemical process [18–20]. With respect to the modified electrodes, an apparent difference in the impedance spectra was observed in Fig. 3B. The Nyquist complex plane plots of both s-BLM with and without doping of Pt nanoparticles were characterized by part of a single semicircle in high-frequency domain, which was in agreement with the expectation from their equivalent circuit. Values of C_m of s-BLM without doping Pt nanoparticles were determined from the complex plot using the Randles equivalent circuit to be 0.39 ± 0.01 μF/cm^2, which were comparable

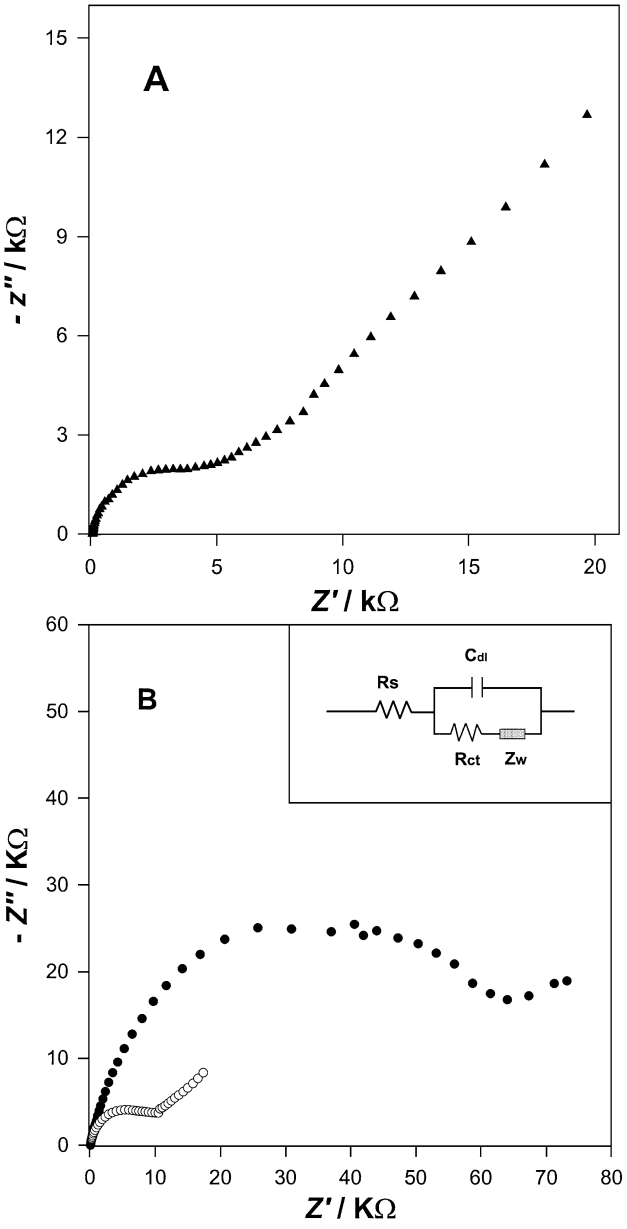

Fig. 3. Nyquist complex plane impedance plots in 10 mM $K_3[Fe(CN)_6]$:$K_4[Fe(CN)_6]$ (1:1) mixture containing 0.1 M KCl at (A) bare GC electrode (▲), and (B) DMPC/GC electrode (●) and Pt@DMPC/GC electrode (○), respectively. Insert: Modified Randles equivalent circuit used to model impedance data in the presence of redox couples.

with the published data [17,18,21,22]. After doping with Pt nanoparticles, vales of C_m were changed to 0.44 ± 0.02 μF/cm^2. The values of R_{ct} could also be obtained from the equivalent circuit in Fig. 3B. The values of R_{ct} for DMPC/GC were 2.47 ± 0.03 kΩ cm^2; after doping with Pt nanoparticles, while the values of R_{ct} for Pt@DMPC/GC were changed to 0.37 ± 0.04 kΩ cm^2. We concluded that doping of Pt nanoparticles in s-BLM caused the membrane capacitance to increase and the membrane resistance to decrease.

3.4. AFM and SEM characterization of the surface morphology of the Pt@DMPC/GC and Pt/GC, respectively

AFM uses atomic or molecular interaction forces between the cantilever and the sample as probe. It is a powerful technique for imaging the surface on a molecular scale without the requirement of conducting samples. This technique has been extensively used to study the various structures of phospholipids, such as molecular resolution and macroscale images of phospholipids, by different preparation techniques [23,24], the morphologies of phospholipids under various conditions and the phospholipids in interaction with proteins and DNA [25,26]. More recently, AFM was used to study the mechanism and the kinetics of the formation and the growth of the phospholipids monolayer and bilayers on solid support [27]. In this study, we used AFM to characterize the morphology for nanostructured Pt-lipid bilayer composite.

Fig. 4A is a typical AFM image of the surface for DMPC/GC. Before the deposition of Pt nanoparticles, the topography of DMPC/GC is relative smooth with a height variation of about 20 nm. Incorporation of Pt nanoparticles is manifested by the formation of numerous domains with a height variation of around 40 nm as shown in Fig. 4B. These images provide a direct verification of Pt nanoparticles deposited through the lipid membranes. It reveals that a portion of the Pt nanoparticles embedded in the lipid membrane extend from the membrane by as much as 20 nm (compare Fig. 4A with Fig. 4B). Furthermore, Pt nanoparticles were distributed in all locations of the lipid membrane. For comparison, Pt particles were electrochemically deposited directly at bare GC electrode. The diameters of Pt particles at the surface of the bare GC without s-BLMs range from 200 to 430 nm as shown in the SEM image of Fig. 4C. The diameters of Pt particles could be 10 times larger than those of Pt nanoparticles deposited through the lipid membranes.

3.5. Current response, reproducibility and stability of the enzyme electrode, GOx/Pt@DMPC/GC as a biosensor to glucose

We immersed the electrode modified with BLM in 2 mg/ml GOx solution for 12 h to allow GOx incorporated into s-BLM; then we tested the current response of the enzyme electrode to glucose. A current–time plot (applied potential +0.40 V) of the enzyme electrodes with the addition of 0.1 mM glucose is demonstrated in Fig. 5. When blank PBS was added into the solution, there was no response for all three electrodes. However, when 1.0 mM glucose was added into the buffer solution, only GOx/Pt@DMPC/GC caused an oxidation current response as shown in Fig. 5A(c). The response time (reaching 90% of the maximum response) was 17 s, which indicated a fast diffusional process and a high activity of the GOx in this nanoparticle lipid composite.

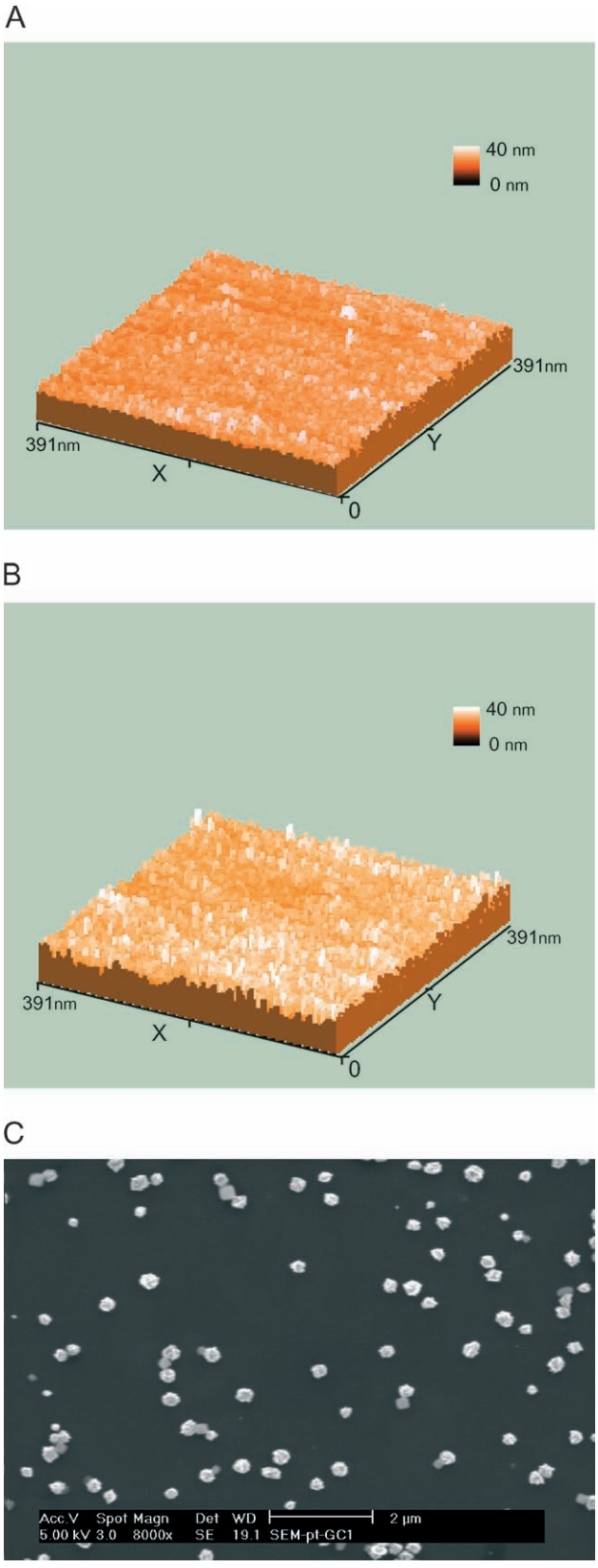

Fig. 4. AFM images of (A) DMPC/GC, (B) Pt[@]DMPC/GC and SEM image of (C) Pt/GC.

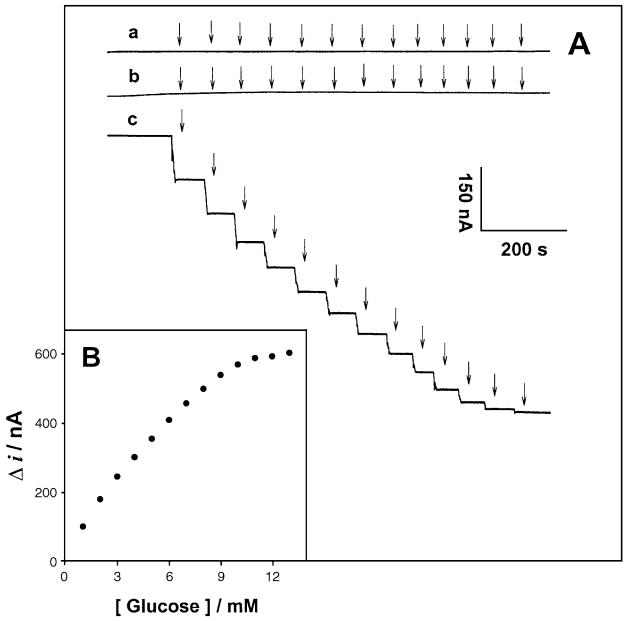

Fig. 5. (A) Typical current–time response of (a) GOx/Pt/GC, (b) GOx/DMPC/GC, or (c) GOx/Pt[@]DMPC/GC enzyme electrode with the injection of 1.0 mM glucose in PBS, respectively. Applied potential, +0.40 V. (B) Calibration curve of GOx/Pt[@]DMPC/GC. Experimental conditions are the same as those of A.

The calibration curve of the GOx/Pt[@]DMPC/GC is shown in Fig. 5B. The linear range of glucose concentration spans between 0.1 and 9.0 mM with a correlation coefficient of 0.9768. The enzyme electrode had a detection limit of 0.04 mM at a signal-to-noise ratio of 3. The reproducibility was examined with the addition of 1.0 mM glucose using the same enzyme electrode, and the relative standard deviation was 3.1% ($n = 9$).

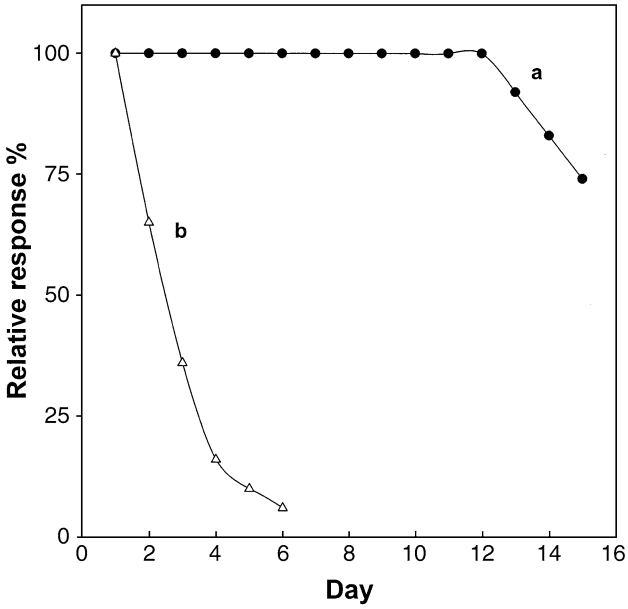

Fig. 6. Stability of GOx/Pt[@]DMPC/GC stored at (a) 4 °C in air or (b) 4 °C in PBS. Other conditions are the same as those of Fig. 5A.

The stability of the enzyme electrode was tested by storing the electrode in the refrigerator at 4 °C. When storing at 4 °C in air, there was no apparent decrease in the response to 1 mM glucose within 12 days [Fig. 6(a)]. The stability demonstrated that Pt nanoparticle-doped s-BLM retained a biomimetic environment on the surface of the GC electrode to maintain the activity of the glucose oxidase. However, when continuously soaking the electrode in PBS at 4 °C [Fig. 6(b)], the current response to 1 mM glucose decreased quickly within 2 days. The fast decrease of the current response may be attributed to the lost of GOx from the lipid membrane in constant solution phase.

4. Discussion

The extreme fragility of the conventional BLM (c-BLM) seriously limits its utility as a practical tool because it cannot be easily produced and will not endure rugged laboratory handling. This problem of fragility was finally overcome by forming BLMs on solid supports [1–3], which substantially improve the stability. Because the s-BLMs have been proven to be very useful and easy to work in the field of membrane research and has solved the shortcomings of the c-BLM, stable s-BLMs on solid substrates are of practical and scientific interest, especially the s-BLMs based on glassy carbon in electrochemical investigation. Upon further modification of the BLM by embedding appropriate receptors, their counterparts in the bathing solution may be selectively detected, thereby affirming the principle of ligand–receptor interactions [5–7,9–11,16–19,21,28,29]. In such a biomimetic approach, a lipid bilayer is used to construct electrochemical biosensor [10]. The functions of biomembranes are mediated by specific modifiers, which can improve the specificity and the selectivity of the biosensors. In the present study, Pt nanoparticles were electrochemically deposited through the lipid films to improve the functions of s-BLMs. The incorporation of Pt particles through the s-BLMs resulted in a unique nanoelectrode array which not only enhanced the capacitance and decreased the resistance of s-BLMs, but also increased the sensitivity for s-BLMs in electrocatalyzing the reduction of O_2 as well as rendering s-BLMs as glucose sensor when GOx was incorporated into s-BLMs.

The immobilization of Pt nanoparticles indicates that the Pt nanoparticles grow in nanoscale voids in the s-BLMs through which the underlying GC electrode is connected to the circuit. This implicates that the Pt nanoparticles serve as nanoscale conductors that are electrically connected to the GC substrate and that penetrate through the s-BLMs to distances of tens of nanometers beyond the membrane surface as shown by the surface morphology of the atomic force image (Fig. 4B). The outer surface is where one would expect the GOx to exist in the experiments that catalyze the reduction of glucose in buffer solution. The result has shown that the nanoscale electrodes penetrate through an insulator of lipid membranes to monitor events at their surface. The advantage and novelty of this device is an electrode system at the nanoscale that can probe through the membrane to investigate the molecular interaction and recognition at the external surface of s-BLMs.

There have been numerous reports within the last decade on self-assembled molecules and supported membranes and their closely related systems such as Langmuir–Blodgett films [1,4,18,19,30–32]. The sustained and continued interest is due to the fact that BLMs provide a natural environment for embedding of proteins, pigments and other membrane constituents with little denaturation. The key successful construction of BLM-based sensors is the ability to embed functional molecules into the lipid bilayer environment which is hydrophobic, liquid-like and self-organizing. The essential idea is to use the s-BLM as a backdrop for the incorporation of materials of interest as well as to use it for signal transduction. To improve the properties of BLM for practical application, many compounds, such as semiconducting nanoparticles, polymeric materials and fullerenes, have been successfully incorporated into BLM [33]. In conclusion, we have shown that: (1) Pt nanoparticles can be successfully deposited through BLM as a novel nanoelectrode array system; and (2) s-BLM with doping of Pt nanoparticles retains a biocompatible microenvironment for enzyme, such as GOx, to maintain its active conformation for catalytic reaction. We propose that other metallic nanoparticles, such as Cu, Pd, Rh and Au, may be deposited through s-BLM. In addition, supported lipid biomembrane can also be employed for embedding a variety of compounds such as peptides, enzymes, antibodies, receptors, ionphores and redox species in the detection of their respective counterparts such as antigens, hormones, ions and electron donors or acceptors [1,4]. The nanostructured metallic lipid bilayer composite we developed here may provide a rationale for the construction of ligand-specific biosensors.

Acknowledgements

This work is supported by the Academic Research Grant of the National University of Singapore R-377-000-015-112 to F.-S. S.

References

[1] H.T. Tien, A.L. Ottova, Membrane Biophysics: As Viewed from Experimental Bilayer Lipid Membranes (Planar Lipid Bilayers and Spherical Liposomes), Elsevier, Amsterdam, 2000.
[2] O. Purrucker, H. Hillebrandt, K. Adlkofer, M. Tanaka, Deposition of highly resistive lipid bilayer on silicon–silicon dioxide electrode and incorporation of gramicidin studied by ac impedance spectroscopy, Electrochim. Acta 47 (2001) 791–798.
[3] G. Wiegand, N. Arribas-Layton, H. Hillebrandt, E. Sackmann, P. Wagner, Electrical properties of supported lipid bilayer membranes, J. Phys. Chem., B 106 (2002) 4245–4254.
[4] R. Guidelli, G. Aloisi, L. Becucci, A. Dolfi, M.R. Moncelli, F.T. Buoninsegni, New directions and challenges in electrochemistry–bi-

oelectrochemistry at metal/water interfaces, J. Electroanal. Chem. 504 (2001) 1–28.
[5] M. Eray, N.S. Dogan, A micromachined polymide aperture for stable bilayer-lipid membrane (BLMs), IEEE Trans. Electron. Dev. 40 (1993) 2137–2138.
[6] A. Ottova, V. Tvarozek, J. Racek, J. Sabo, W. Ziegler, T. Hianik, H.T. Tien, Self-assembled BLMs: biomembrane models and biosensor applications, Supramol. Sci. 4 (1997) 101–112.
[7] H.T. Tien, Z. Salamon, J. Kutnik, P. Krysinski, J. Kotowski, D. Ledermann, T. Janas, Bilayer lipid-membrane (BLM)—an experimental system for biomolecular electronic device development, J. Mol. Electron. 4 (1988) S1–S30.
[8] X.K. Zhao, S. Baral, J.H. Fendler, Electrochemical characterization of bilayer lipid-membrane semiconductor junctions, J. Phys. Chem. 94 (1990) 2043–2052.
[9] H. Gao, J. Feng, G.A. Luo, A.L. Ottova, H.T. Tien, Some electrochemical features of supported bilayer lipid membranes, Electroanalysis 13 (2001) 49–53.
[10] Z. Wu, B. Wang, Z. Cheng, X. Yang, S. Dong, E. Wang, A facile approach to immobilize protein for biosensor: self-assembled supported bilayer lipid membranes on glassy carbon electrode, Biosens. Bioelectron. 16 (2001) 47–52.
[11] H. Haas, G. Lamura, A. GliozziHaas, Improvement of the quality of self assembled bilayer lipid membranes by using a negative potential, Bioelectrochemistry 54 (2001) 1–10.
[12] C. Amatore, J.M. Saveant, D. Tessier, Charge transfer at partially blocked surfaces: a model for the case of microscopic active and inactive sites, J. Electroanal. Chem. 147 (1983) 39–51.
[13] P. Diao, D. Jiang, X. Cui, D. Gu, R. Tong, B. Zhong, Unmodified supported thiol lipid bilayers: studies of structural disorder and conducting mechanism by cyclic voltammetry and AC impedance, Bioelectrochem. Bioenerg. 48 (1999) 469–475.
[14] T.C. Kuo, R.L. McCreery, Surface chemistry and electron-transfer kinetics of hydrogen-modified glassy carbon electrodes, Anal. Chem. 71 (1999) 1553–1560.
[15] R. Rice, C. Allred, R.L. McCreery, Fast heterogeneous electron-transfer rates for glassy-carbon electrodes without polishing or activation procedures, J. Electroanal. Chem. 263 (1989) 163–169.
[16] P. Krysiński, M.R. Moncelli, F. Tadini-Buoninsegni, A voltammetric study of monolayer and bilayers self-assembled on metal electrodes, Electrochim. Acta 45 (2000) 1885–1892.
[17] J.S. Ye, A. Ottova, H.T. Tien, F.S. Sheu, Nitric oxide enhances the capacitance of self-assembled, supported bilayer lipid membranes, Electrochem. Commun. 3 (2001) 580–584.
[18] D. Ivnitski, E. Wilkins, H.T. Tien, A. Ottova, Electrochemical biosensor based on supported planar lipid bilayers for fast detection of pathogenic bacteria, Electrochem. Commun. 2 (2000) 457–460.
[19] Y.L. Zhang, H.X. Shen, C.X. Zhang, A. Ottova, H.T. Tien, The study on the interaction of DNA with hemin and the detection of DNA using the salt bridge supported bilayer lipid membrane system, Electrochim. Acta 46 (2001) 1251–1257.
[20] X.M. Ren, P.G. Pickup, An impedance study of electron transport and electron transfer in composite polypyrrole plus polystyrenesulphonate films, J. Electroanal. Chem. 420 (1997) 251–257.
[21] P. Diao, D. Jiang, X. Cui, D. Gu, R. Tong, B. Zhong, Cyclic voltammetry and ac impedance studies of Ca^{2+}-induced ion channels on Pt-BLM, Bioelectrochem. Bioenerg. 45 (1998) 173–179.
[22] A.L. Plant, M. Gueguetchkeri, W. Yap, Supported phospholipid/alkanethiol biomimetic membranes-insulating properties, Biophys. J. 67 (1994) 1126–1133.
[23] S. Singh, D.J. Keller, Atomic force microscopy of supported planar membrane bilayers, Biophys. J. 60 (1991) 1401–1410.
[24] U. Muscatello, G. Valdre, U. Valdre, Atomic force microscopy observations of acyl chains in phospholipids, J. Microsc. 182 (1996) 200–207.
[25] J.D. Burgess, V.W. Jones, M.D. Porter, M.C. Rhoten, F.M. Hawkridge, Scanning force microscopy images of cytochrome *c* oxidase immobilized in an electrode-supported lipid bilayer membrane, Langmuir 14 (1998) 6628–6631.
[26] Y. Fang, J. Yang, Two-dimensional condensation of DNA molecules on cationic lipid membranes, J. Phys. Chem. 101 (1997) 441–449.
[27] Z.Y. Tang, W.G. Jing, E.K. Wang, Self-assembled monolayer growth of phospholipids on hydrophobic surface toward mimetic biomembranes: scanning probe microscopy study, Langmuir 16 (2000) 1696–1702.
[28] K. Asaka, A. Ottova, H.T. Tien, Mediated electron transfer across supported bilayer lipid membrane (s-BLM), Thin Solid Films 354 (1999) 201–207.
[29] J. Sabo, A. Ottova, G. Laputkova, M. Legin, L. Vojcikova, H.T. Tien, A combined AC–DC method for investigating supported bilayer lipid membranes, Thin Solid Films 306 (1997) 112–118.
[30] W. Schulmann, S.P. Heyn, H.E. Gaub, Immobilization of enzymes on Langmuir–Blodgett films via a membrane-bound receptor: possible application for amperometric biosensors, Adv. Mater. 3 (1991) 388–391.
[31] K.T. Kinnear, H.G. Monbouquett, Direct electron transfer to *Escherichia-coli* fumarate reductase in self-assembled alkanethiol monolayers on gold electrodes, Langmuir 9 (1993) 2255–2257.
[32] T. Miyashita, Y. Ito, Spreading behavior of polymerizable monolayers of acrylamides with double alkyl chains and polymerization of the LB films, Thin Solid Films 260 (1995) 217–221.
[33] H.T. Tien, A.L. Ottova, Supported planar lipid bilayers (s-BLMs) as electrochemical biosensors, Electrochim. Acta 43 (1998) 3587–3610.